Contents

Introduction

The study of atomic nuclei forms the bridge between fundamental areas of theoretical and computational physics and nuclear engineering. While experimental data has provided over the years invaluable information about nuclear structure, reactions and other important nuclear processes, the predictions provided by a theoretical understanding although still unsatisfactory due to the extremely vast landscape of nuclear physics, are essential for nuclear engineering.

In particular, fission reactions, which are of the utmost importance in nuclear engineering, are still poorly understood, models relying on mean-fields and empirical descriptions of the nucleus are too coarse to help us understand the exact physical process, let alone make numerically accurate predictions, which is a major challenge for the simulation of new generation nuclear reactors, which use neutron rich nuclei and fuel materials much less understood than the traditional thermal reactors.

In this regard, the most successful approach to the microscopic description of nuclei, is certainly the exact many-body system, which starting from the interactions among nucleons, aims at building a complete description of the nucleus. At the moment, there are two competing frameworks that try to tackle the problem,

i the *ab-initio* approach, where the interaction is in principle exact, derived from controlled approximations of quantum chromodynamics; and

ii the use of effective interactions and nuclear Density Functional Theory.

Ab-initio methods, while technically speaking more rigorous, are still limited as of now, since they can only account for light, spherical nuclei. Energy density functionals and effective interactions, such as the Skyrme force, on the other hand are more flexible and less computationally expensive enabling a much wider representation of nuclei across the whole chart, including heavy nuclei, which are of crucial importance in nuclear engineering.

D Vautherin and D M Brink laid the foundations of the nuclear Hartree-Fock theory using the Skyrme interaction in 1972, through spherically symmetric calculations, which are unable to account for nuclear deformations, essential for nuclei far from magic numbers and

in the heavy region. Over the years, thanks to the increase in computational performance of modern hardware, codes that are able to represent more coordinates have been written, mainly using basis expansions of the harmonic oscillator, which presents many downsides, such as the inability to represent superdeformed states or nuclei near drip lines.

In the past twenty years, the use of meshes to better account for such extremal cases has been introduced, still assuming certain simplifications, such as plane reflections, cylindrical symmetries and so on. The use of fully unconstrained Hartree-Fock methods, of critical importance for exotic deformations, is still a novel endevour that only a handful of implementations have tackled, due to the high computational cost.

The aim of this work is to explore a new computational approach, the General Conjugate Gradient method, to efficiently solve spatially unconstrained Skyrme functionals. This thesis is organised as follows:

- In chapter 1, a short, comprehensive introduction to nuclear physics is given, as to prime the reader on the essential physical properties of atomic nuclei, starting from phenomenological facts and empirical models. A formal description of nuclear deformations and fission is also given, to highlight the importance of symmetry breaking.
- In chapter 2, a short summary of the methods used in this thesis is given, both theoretical and numerical, as well as a state-of-the-art comparison with other codes.
- In chapter 3, the theoretical framework used in the present work is reviewed, by introducing aspects of Hartree-Fock theory, Density Functional Theory and the effective interaction used in this work.
- In chapter 4, the numerical methods used in this work are presented, along with actual implementations of them in writing the code.
- In chapter 5, results for the spherically symmetric case are presented as a way of benchmarking the new implementation of this thesis, along with a description of the main physical quantities we compare.
- In chapter 6, benchmarks for the deformed nucleus ^{24}Mg are shown, after which novel results regarding... are presented.

1 | Nuclear structure and deformations

In this chapter, a concise introduction to nuclear physics is provided, as a way to understand the essential physical properties of the system under study. First, in section 1.1, we will review the main empirical facts about nuclides, such as particle density distribuion and binding energies and the simple phenomenological models historically employed to describe them. Moving on to more advanced topics, that are able to complete the general description of nuclear structure, which are nuclear pairing in section 1.2 and nuclear deformations in section 1.3.
Lastly, in section 1.4, we will overview the nuclear fission process, by deriving a simple model to describe it and discussing the importance of exotic deformations to accurately describe it.

1.1. Nuclear structure models

The study of low energy hadron physics, has always been a challenging task. This is due to the known fact that the strong force, which is responsible for the attraction between the nucleons in a nuclei, is not perturbative at low energies, as opposed to the atomic case for the Coulomb interaction.

1.1.1. Phenomenology of the NN interaction

It is possible to obtain a good insight on the nuclear structure, by using empirical data obtained experimentally on the more macroscopic properties of nuclei, such as the binding energy and the particle density.

Binding energies

Let us start by the omnipresent physical quantity that is the binding energy of a nucleus. We can define it as the mass defect of the nucleus with respect to the constituents –

protons and neutrons – isolated from eachother. If Z is the number of protons, N the number of neutrons, and $A = N + Z$ the nuclear mass, then the binding energy E_B is given by

$$E_B = (Zm_p + Nm_n - M)c^2 \tag{1.1}$$

where m_p is the proton mass, m_n the neutron mass, and M the nucleus mass.
In figure 1.1, the binding energy per nucleon E_B/A of nuclei as a function of A is plotted. As shown in the figure, the binding energy per nucleon rapidly saturates and stalls around 7 MeV just after $A = 4$, this striking behaviour is due to nucleons interacting only with near neighbours, since the strong force is a short-range interaction, otherwise, the trend would follow a behaviour of $A(A-1)$ as in the Coulomb interaction case.

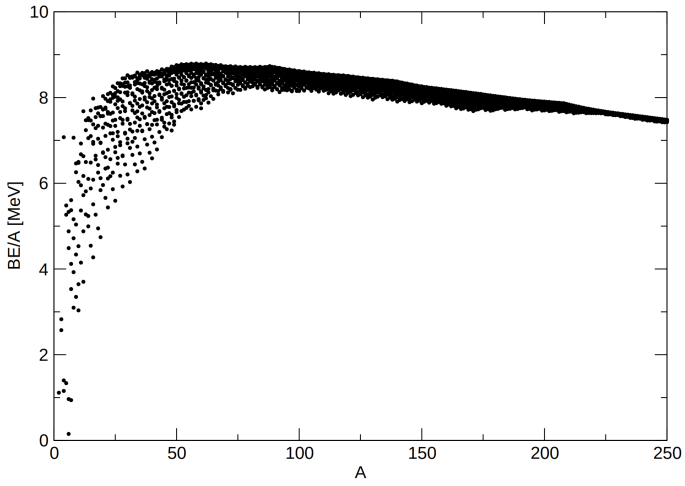

Figure 1.1: Binding energy per nucleon as a function of A. Due to the short range of the strong force, this value saturates around 7 MeV, with a steady, dim decrease after ^{56}Fe.

Nuclear density

An important aspect of nuclear phenomenology which can be easily obtained through electron scattering experiments [33] is the nuclear density. It can be very well represented by a Fermi-like distribution, which reads

$$\rho(r) = \frac{\rho_0}{1 + e^{\frac{r-R_0}{a}}}, \tag{1.2}$$

where R_0 is the nuclear radius, which can be parametrized as $R_0 \approx 1.2A^{1/3}$, and a is the diffusivity, whose value determines how sharp the density drops from its saturation value $\approx \rho_0$ to ≈ 0. The saturation density ρ_0 is generally universal for all nuclei, amounting to ≈ 0.16 fm^{-3}.

1.1.2. Nuclear models

The formal description of nuclear structure has been proven to be a difficult task over the years. Due to the extremely rich phenomenology of nuclei and the challenges brought by the strong force, as we shall see, many models and further approximations to give a satisfactory description of all nuclides have been proposed.

Liquid drop model

One, if not the first successful model, is the liquid drop model. It is based on the assumption that the nucleus behaves as a liquid droplet, where forces among consituents tend to saturate. This hypothesis, formulated by G. Gamow, culminated in the formalization of the semi-empirical mass formula (SEMF) by N. Bohr and C. F. von Weizsäcker in 1935 [74], which reads

$$E_B = a_V A - a_S A^{2/3} - a_C \frac{Z(Z-1)}{A^{1/3}} - a_A \frac{(N-Z)^2}{A} + \delta_P \tag{1.3}$$

where E_B is the binding energy of the nucleus. Each term has a different physical meaning:

- $a_V A$ is the volume energy of the nucleus, given by the approximately constant binding energy per nucleon, which makes the total energy roughly proportional to A;
- $a_S A^{2/3}$ is the surface energy, a correction to the volume energy due to outer nucleons interacting with fewer nucleons than those in the inner bulk;
- $a_C Z(Z-1)/A^{1/3}$ is the approximation to the Coulomb energy repulsion of the nucleus, assuming the protons are uniformly distributed;
- $a_A(N-Z)^2/A$ is the asymmetry energy, which is due to the Pauli exclusion principle, since protons and neutrons occupy their respective states, a high imbalance of one species or the other implies loosely bound nucleons, thus a higher energy contribution of those states; and
- δ_P refers to the pairing energy of the nucleus, whose parametrization and physical significance will be later discussed in section 1.2.

The SEMF can be fitted on current data to get a good estimate of binding energies [5], but it still lacks the ability of describing many aspects of nuclear structure, mainly, the nuclear shell structure, which can account for magic numbers and nuclear deformations.

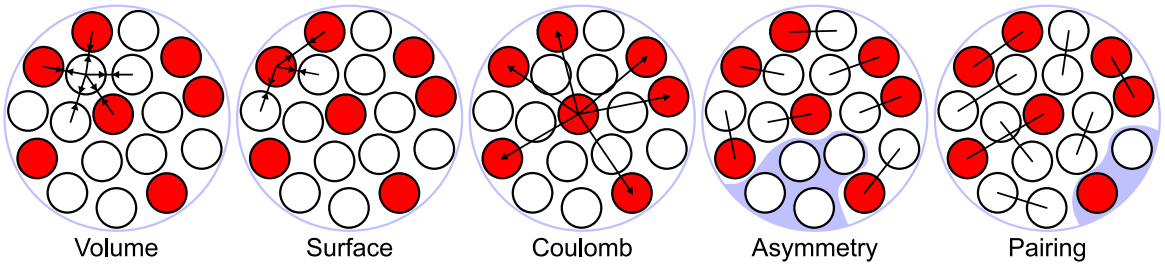

Figure 1.2: Visual representation of the liquid drop model from [28]

Shell corrections

Describing the nucleus through a shell model would account for the quantum mechanical nature of the system, unfortunately, unlike the 'atomic' case, we don't have a source of the field to which nucleons are sucjected to, since it's generated by the nucleons themselves; nonetheless, the formulation of an empirical potential which reproduces experimental data has been proven to be successful in providing useful corrections to the liquid drop model.

The so called Woods-Saxon potential is an empirical field used for modelling the average field to which an independent nucleon would feel in a nucleus. It can take different parametrizations depending on the data that one wants to reproduce. It is formulated as to follow the shape of the nuclear density (1.2), and it reads

$$U(\boldsymbol{r}) = -\frac{U_0(A,N)}{1+e^{\frac{r-R}{a}}} \tag{1.4}$$

where U_0 is the potential depth

$$U_0(A,N) = U_0\left(1 \pm \kappa\frac{2N-A}{A}\right), \tag{1.5}$$

the $+$ and $-$ signs refer to protons and neutrons respectively. R refers to the radius of the nuclear surface, generally parametrized as

$$R = r_0 A^{1/3} \tag{1.6}$$

and a is the surface diffuseness, as in the density expression (1.2).

Spin-orbit coupling The success of the shell model is mainly due to the possibility of accounting for spin-orbit coupling, which is included through a term that reads

$$U_{\mathrm{LS}}(\boldsymbol{r}) = U_0^{\mathrm{LS}} \left(\frac{r_0}{\hbar}\right)^2 \frac{1}{r}\frac{\mathrm{d}}{\mathrm{d}r}\left(\frac{1}{1+e^{\frac{r-R}{a}}}\right). \tag{1.7}$$

Coulomb interaction In the spherical case, the coulomb interaction can be taken as the energy potential produced by a sphere of charge Z and radius R, which reads

$$U_{\mathrm{C}}(r) = Ze^2 \begin{cases} \frac{3-(r/R)^2}{2R} & r \leq R, \\ \frac{1}{r} & r > R. \end{cases} \tag{1.8}$$

The complete Hamiltonian then reads

$$\hat{H} = \hat{T} + U + U_{\mathrm{LS}} + U_C, \tag{1.9}$$

where U_C is present only when solving for the proton shells. The solution to the eigenvalue problem $\hat{H}\psi = E\psi$ is of the form

$$\psi_{nljm_j} = \frac{u_{nl}(r)}{r}[Y_{nl}(\hat{\boldsymbol{r}}) \otimes \chi_{1/2}]_{jm_j} \tag{1.10}$$

where $Y_{nl}(\hat{\boldsymbol{r}})$ is the spherical harmonic function of degree l and order m, the $\hat{r}$ notation is used to denote dependence on the azimuthal and polar angles of $\boldsymbol{r}$, $\otimes$ takes the meaning of the angular momentum coupling with the spinor $\chi_{1/2}$, and $u_{nl}(r)$ satisfies the reduced Schrödinger equation

$$\left(-\frac{\hbar^2}{2m}\frac{\mathrm{d}^2}{\mathrm{d}r^2} + \frac{\hbar l(l+1)}{2mr^2} + U(r)\right)u_{nl} = Eu_{nl}. \tag{1.11}$$

The effect of the spin-orbit coupling U_{LS} and the Coulomb repulsion U_C can be accounted for by using first order perturbation theory.

Harmonic oscillator

A small digression on the harmonic oscillator is in order. The solution of the spherical potential

$$U_{\mathrm{HO}}(\boldsymbol{r}) = \frac{1}{2}m\omega^2 r^2, \tag{1.12}$$

produces the spherical harmonic oscillator basis, which is very similar to the basis one would get solving for the Woods-Saxon potential, provided that ω is taken as $41/A^{1/3}$ MeV.

As a matter of fact, the harmonic oscillator basis is often used to perform calculations in nuclear physics. We will see in section 4.3 that a harmonic oscillator basis is used as starting guess for the numerical solution of a Woods-Saxon potential.

Shell structure

A graphical representation of the shells for a harmonic oscillator is shown in figure 1.3, where the contribution of the spin-orbit coupling is also accounted for; unlike the atomic case, shells whose total angular momentum is higher are lowered in energy, viceversa for lower total angular momentum.

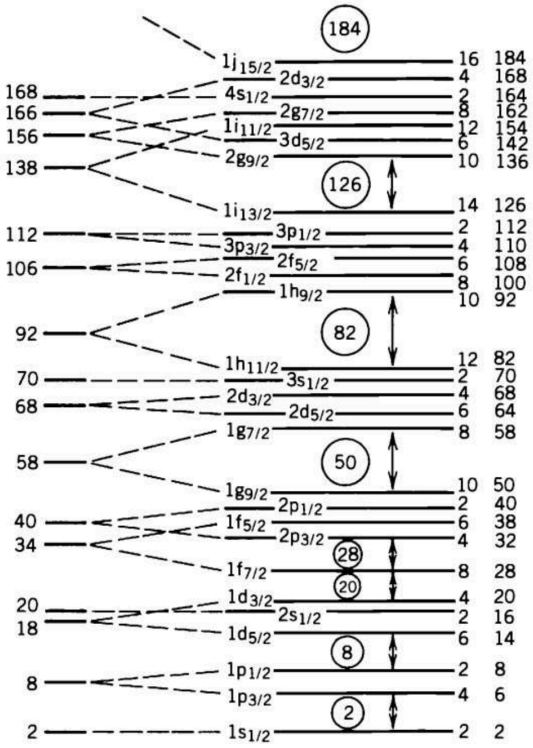

Figure 1.3: Graphical representation of a harmonic oscillator shells, together with the spin-orbit coupling. Shells whose total angular momentum is higher are lowered in energy, viceversa for lower total angular momentum.

1.2. Nuclear pairing

In the semi-empirical mass formula (1.3), the δ_p term can be parametrised as

$$\delta_p = \begin{cases} +\delta_0 & \text{if N and Z are even,} \\ 0 & \text{if A is odd,} \\ -\delta_0 & \text{if N and Z are odd,} \end{cases} \tag{1.13}$$

hence having an even number of neutrons and/or protons increases the binding energy of the nucleus. A common choice for δ_0 is

$$\delta_0 = 12A^{1/2} \text{ MeV}.$$

This is a phenomena closely related to superconductivity, as nucleons of the same type form pairs that lie in higher energy states. An experimental evidence of this fact is knwon as odd-even staggering, where the separation energy

$$S_n = E_B(A, Z) - E_B(A-1, Z), \tag{1.14}$$

is higher for even A, an increase that corresponds to the energy necessary to break a pair. We will see in section 3.2 the two main methods to account for pairing at a microsopic level.

1.3. Nuclear deformations

We shall now give a description of the nuclear shape in a formal framework. We will start by expanding the nuclear radius in terms of spherical harmonics, so that we can truncate and omit terms to describe certain configurations of the nucleus, so that we are able to illustrate the simple case of an axial quadrupole deformation. After that, we will briefly discuss the more general case of trixial, octupole, and parity breaking configurations.

1.3.1. Quadrupole deformation

Assuming the nuclear volume to be evaluated as

$$V(A) = \frac{4}{3}\pi R^3 \tag{1.15}$$

Let us suppose to consider variations of the nuclear radius R in terms of spherical harmonics

$$R(\theta,\phi) = R_0\left[1 + \sum_{\lambda\mu} \alpha_{\lambda\mu}\, Y_{\lambda\mu}(\theta,\phi)\right] \tag{1.16}$$

where the moments $\alpha_{\lambda\mu}$ defined as

$$\alpha_{\lambda\mu} = \int Y^*_{\lambda\mu}(\theta,\phi) R(\theta,\phi) d\Omega, \tag{1.17}$$

are considered small, in the sense that $|\alpha_{\lambda\mu}|^2 \ll |\alpha_{\lambda\mu}|$ as to conserve the volume in equation (1.15). We have that Y_{00} is constant, so its moment does not provide additional information to the constant radius. We can set $\alpha_{00} = 0$. Since Y_{10}, Y_{11} and Y_{1-1} are odd for $\theta + \pi$ and $\phi + \pi$, we have that $\alpha_{1\mu}$ vanishes in a reference frame in which the centre of mass is at the origin.
Now, let us consider only $\alpha_{2\mu}$ coefficients and neglect higher degree terms, so that the deformation is purely quadrupolar, then the radius reads

$$R(\theta,\phi) = R_0\left[1 + \sum_{\mu=-2}^{2} \alpha_{2\mu}\, Y_{2\mu}(\theta,\phi)\right]. \tag{1.18}$$

If we assume to be in the reference frame in which the inertia tensor, proportional to the coefficients $\alpha_{2\mu}$, is diagonal, which is known as intrinsic frame, then the sum

$$\alpha_{21} Y^*_{21} + \alpha_{2-1} Y^*_{2-1}$$

vanishes. Since R is a real valued function, we have the relation

$$\alpha_{\lambda\mu} Y_{\lambda\mu} + \alpha_{\lambda-\mu} Y_{\lambda-\mu} = 2\,\mathrm{Re}\{\alpha_{\lambda\mu} Y_{\lambda\mu}\}, \tag{1.19}$$

as a consequence, the resulting expansion reads

$$\begin{aligned} R(\theta,\phi) &= R_0\left[1 + a_{20}Y_{20} + 2\,\mathrm{Re}\{a_{22}Y_{22}\}\right] \\ &= R_0\left[1 + \sqrt{\frac{5}{16\pi}}\left(a_{20}(3\cos^2\theta - 1) + 2a_{22}\sqrt{3}\sin^2\theta(\cos^2\phi - \sin^2\phi)\right)\right]. \end{aligned} \tag{1.20}$$

If we perform the substitution

$$a_{20} = \beta\cos(\gamma) \tag{1.21}$$

$$a_{22} = \beta\sin(\gamma) \tag{1.22}$$

and express the variation of R along the cartesian axes, we get

$$R_x - R_0 = \delta R_x = \sqrt{\frac{5}{4\pi}}\beta R_0 \cos\left(\gamma - \frac{2\pi}{3}\right), \tag{1.23}$$

$$R_y - R_0 = \delta R_y = \sqrt{\frac{5}{4\pi}}\beta R_0 \cos\left(\gamma + \frac{2\pi}{3}\right), \tag{1.24}$$

$$R_z - R_0 = \delta R_z = \sqrt{\frac{5}{4\pi}}\beta R_0 \cos\gamma. \tag{1.25}$$

Assuming the value of β to always be positive, in the case $\gamma = 0$, $\delta R_x = \delta R_y < \delta R_z$, meaning the nucleus is in a *prolate* configuration; while in the case of $\gamma = \pi/3$, $\delta R_x = \delta R_y > \delta R_z$, meaning the nucleus has an *oblate* shape. A general convention is to write β with a negative sign in the oblate case, and a positive sign in the prolate case.
By using trigonometric identities, it is trivial to show that unique shapes are found only for $\gamma \in [0; \pi/3]$, if γ takes a value different from 0 or $\pi/3$, the shape is said to be triaxial, meaning $\delta R_z \neq \delta R_x \neq \delta R_y$, the nucleus has no more rotational symmetries and is only symmetric for reflections along the (x, y), (x, z) and (y, z) planes, which also induces parity symmetry.

1.3.2. Nilsson model

To understand the effect on single-particle motion of a deformed potential, we can consider the case of an axially deformed harmonic oscillator potential, for which $\omega_z \neq \omega_x = \omega_y = \omega_\perp$, meaning the oscillator frequency takes on a different value on the z axis than in the x and y axes.
To treat the deformation perturbatively, we can assume that the various frequencies deviate from the unperturbed $\omega_0 = 41/A^{1/3}$ MeV, in which case they may read

$$\omega_z = \omega_0 - \frac{2}{3}\varepsilon, \tag{1.26}$$

$$\omega_\perp = \omega_0 + \frac{1}{3}\varepsilon, \tag{1.27}$$

this definition of the frequencies satisfies the conservation of volume, at lowest order in ε, assumed to hold for

$$\omega_0^3 = \omega_z \omega_\perp^2. \tag{1.28}$$

We can thus write the single-particle Hamiltonian in the deformed potential as

$$H = H_0 + \varepsilon H_1, \tag{1.29}$$

$$H_0 = -\frac{\hbar^2}{2m}\nabla^2 + \frac{1}{2}m\omega_0^2 r^2, \tag{1.30}$$

$$\varepsilon H_1 = \frac{1}{3}\omega_0^2\varepsilon(x^2 + y^2 - 2z^2) = -\frac{1}{3}\sqrt{\frac{16\pi}{5}}m\omega_0^2\varepsilon r^2 Y_{20}. \tag{1.31}$$

H_0 is the usual spherical harmonic potential, for which the eigenfunctions, expressed through the usual quantum numbers $|nljm_j\rangle$ are known. Assuming ε to be small, we can evaluate the first order correction of H_1 to the system, which reads

$$\Delta E = \langle nljm_j|\, \varepsilon H_1\, |nljm_j\rangle\,, \tag{1.32}$$

$$= -\frac{1}{3}\sqrt{\frac{16\pi}{5}}\varepsilon m\omega_0^2 \int r^2 u_{nl}(r)\, \langle jm_j|\, Y_{20}\, |jm_j\rangle\, dr, \tag{1.33}$$

$$= \frac{\varepsilon}{6}m\omega_0^2 \int r^2 u_{nl}(r)\frac{3m_j^2 - j(j+1)}{j(j+1)}dr, \tag{1.34}$$

thus in the limit of large j, states with the maximum total angular momentum projection m_j are shifted upwards, while states with the minimum m_j are shifted downwards; moreover, eigenstates with $\pm m_j$ are degenerate, as expected by the reflection symmetry of the Hamiltonian if the z axis is inverted.

Adding further empirical terms to reproduce experimental data, and the spin-orbit coupling, results in the formulation of the Nilsson model [50]. In figure 1.4, a graphical representation of the energy levels in the Nilsson model is shown [76].

Deformed Woods-Saxon

Recent studies of deformed nuclei have been carried out using empirical potentials such as deformed Woods-Saxon potentials [25, 35]. In these models, the nuclear shape is expanded as

$$R(\theta) = R_0\left[1 + \sum_{\lambda}^{L}\beta_\lambda Y_{\lambda 0}\right], \tag{1.35}$$

so that the solution is axially symmetric and the problem is reduced to just the (r, θ) coordinates, in which we can write the potential as

$$U_{\mathrm{WS}}(r,\theta) = -\frac{U_0(A,N)}{1 + e^{\frac{r-R(\theta)}{a}}}. \tag{1.36}$$

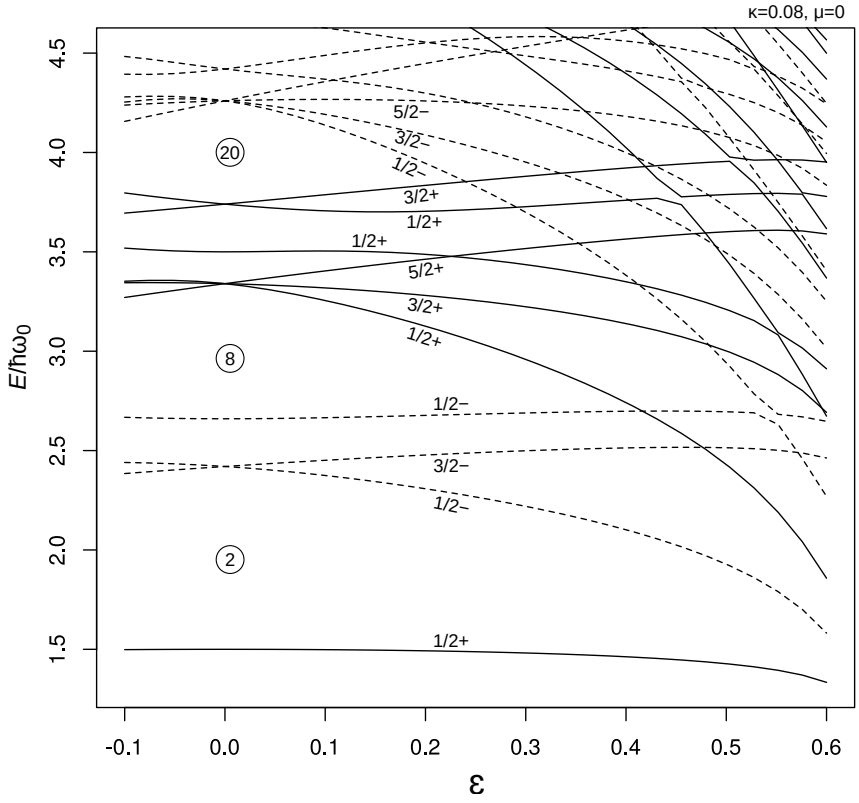

Figure 1.4: Nilsson model energy levels trends, as a function of ε.

1.3.3. Octupole deformations and parity breaking

While quadrupole deformations concern nuclei across the whole chart, octupole deformations are much less common, being found only in heavier nuclei. Under the parity operation $\mathcal{P} : \boldsymbol{r} \mapsto -\boldsymbol{r}$, coefficients of the spherical harmonics transform as

$$\mathcal{P}\alpha_{\lambda\mu} = (-1)^{\lambda}\alpha_{\lambda\mu}, \tag{1.37}$$

hence a nuclear octpuole deformation, whose degree $\lambda = 3$, would break parity symmetry. In figure 1.5 a graphical representation of the spherical harmonics for $\lambda = 3$ and $\mu = 0, 2$ is shown.

1.4. Nuclear fission

Nuclear fission is the process by which a nucleus splits into two – sometimes three – nuclei, whether spontaneously, or induced by a reaction. The physics that governs nuclear fission is the one of many-body, large amplitude collective modes, which elongate the the nuclear shape, until the so called *fission barrier* is surmounted and the path to the energy

Figure 1.5: Graphical representation of possible octupole deformations. On the left, the axially symmetric Y_{30} deformation, on the right, the non-axial octupole deformation Y_{32}.

minimum is one where the nuclei fragments itself.

Spontaneous fission model

It should be ovious that a formal treatment of deformations and collective modes is necessary to give a theoretical description of fission reactions. We can derive a simple spontaneous fission model by studying the effect of a simple axial quadrupole deformation on the semiempirical mass formula 1.3.
Let us assume that the nuclear radius may be expanded, as previously done in section 1.3, as

$$R = R_0[1 + \alpha_{20} Y_{20}]. \tag{1.38}$$

Assuming the nuclear volume is conserved across the fission path, the volume energy will not change. As for the surface energy, its variation can be expressed at the lowest order in α_{20} as

$$\Delta E_{\text{surf}} = E_{\text{surf}} - E_{0,\text{surf}} = E_{0,\text{surf}} \frac{2}{5} \alpha_{20}^2. \tag{1.39}$$

Regarding the Coulomb energy, the variation is given by

$$\Delta E_{\text{coul}} = E_{\text{coul}} - E_{0,\text{coul}} = -E_{0,\text{coul}} \frac{1}{5} \alpha_{20}. \tag{1.40}$$

Since the neutron and proton count does not change, the surface and Coulomb energies are the only contributions to the total energy difference. We can write

$$\Delta E = \frac{2}{5}\alpha_{20}^2 a_s A^{2/3} - \frac{1}{5}\alpha_{20}^2 a_c Z^2 A^{-1/3}, \tag{1.41}$$

if we set equation (1.41) to zero, we get, other than the undeformed solution for $\alpha_{20} = 0$,

$$\frac{Z^2}{A} = \frac{2a_s}{a_c}, \tag{1.42}$$

where the ratio $2a_s/a_c$ amounts to ≈ 50 in typical parametrizations of the SEMF. Equation (1.41), shows that for values of the so called *fissility parameter* Z^2/A larger than 50, the energy change becomes negative, favouring a configuration in which the nucleus fragments due to the spontaneous fission.

1.4.1. Symmetry breaking and microscopic approaches to fission

Microscopic theory

The use of phenomenological macroscopic-microscopic models has long provided valuable insight into fission processes, allowing for the prediction of barrier heights and fragment yields through parametrised shape degrees of freedom and empirical shell corrections [10, 13, 40]. In these models, the total energy is expressed as

$$E_{\text{tot}}(\boldsymbol{q}) = E_{\text{LD}}(\boldsymbol{q}) + \delta E_{\text{shell}}(\boldsymbol{q}) + \delta E_{\text{pair}}(\boldsymbol{q}), \tag{1.43}$$

where E_{LD} is the macroscopic liquid-drop term depending on deformation coordinates $\boldsymbol{q}$, while δE_{shell} and δE_{pair} account for shell and pairing corrections, respectively. While such models reproduce many global observables, they lack a true microscopic foundation. In particular, the collective coordinates $\boldsymbol{q}$ are not derived from the underlying many-body dynamics, and the empirical shell corrections cannot describe the self-consistent rearrangement of the mean field along the fission path.

A more fundamental understanding is achieved within self-consistent mean-field approaches such as the Hartree-Fock or Hartree-Fock-Bogoliubov formalisms. The use of nuclear Density Functional Theory [3, 63] allows one to define a universal EDF $E[\rho, \kappa]$ that encapsulates both mean-field and pairing correlations. The resulting constrained HFB calculations produce the potential energy surface (PES) $E(\boldsymbol{q})$, mapping the energy of the system as a function of collective deformations such as the quadrupole (Q_{20}), octupole (Q_{30}), and triaxial (Q_{22}) moments. The minima and saddle points of this multidimensional PES

determine the fission barriers and shape isomeric states [24, 65].

However, static mean-field approaches are limited by their single-reference character: the HFB vacuum represents only one configuration at a time, typically corresponding to a local minimum of the PES. In the vicinity of the fission barrier, where several configurations with different intrinsic quantum numbers coexist, this approximation breaks down. The wave function should instead be expressed as a superposition of several self-consistent configurations $\{|\Phi(\boldsymbol{q})\rangle\}$, leading to a correlated state of the form

$$|\Psi\rangle = \int f(\boldsymbol{q})\,|\Phi(\boldsymbol{q})\rangle\,d\boldsymbol{q}, \tag{1.44}$$

which is the essence of the *Generator Coordinate Method* (GCM) [30, 55]. The GCM maps the microscopic many-body problem onto a *collective Schrödinger equation* (CSE)

$$\left[-\frac{\hbar^2}{2}\sum_{ij}\frac{\partial}{\partial q_i}B_{ij}(\boldsymbol{q})\frac{\partial}{\partial q_j}+V(\boldsymbol{q})\right]g_k(\boldsymbol{q}) = E_k g_k(\boldsymbol{q}), \tag{1.45}$$

where $B_{ij}(\boldsymbol{q})$ is the collective inertia tensor and $V(\boldsymbol{q})$ the potential energy extracted from constrained HFB. This framework naturally incorporates tunnelling through the barrier and provides access to observables such as fission lifetimes and fragment distributions.

Beyond-mean-field extensions also restore symmetries that are spontaneously broken at the mean-field level. For instance, particle-number, parity, and angular-momentum projection techniques [4, 62] are required to recover good quantum numbers and remove spurious symmetry mixing. In multi-reference DFT [3], these symmetry restorations can be combined with configuration mixing, yielding highly accurate fission barrier calculations.

Unconstrained Calculations and Symmetry Breaking

An equally important aspect of microscopic fission theory is the treatment of spatial symmetries. Historically, many calculations imposed constraints such as axial symmetry or reflection symmetry with respect to a plane to reduce the computational cost of solving the HFB equations. While such restrictions simplify the description of the nucleus, they artificially constrain the fission path and may even prevent the identification of energetically preferred configurations [7, 75]. Fission involves strongly deformed, triaxial, and reflection-asymmetric shapes; the correct description of barrier heights and scission configurations therefore requires breaking as many spatial symmetries as possible.

In the self-consistent mean-field framework, spontaneous symmetry breaking is a feature

rather than a flaw: it allows the system to adopt a deformed intrinsic shape corresponding to a broken rotational or parity symmetry, while the symmetry of the total many-body Hamiltonian is preserved. For example, an axially deformed HFB state violates rotational invariance, but the restoration of this symmetry through angular-momentum projection recovers the correct laboratory-frame properties. Similarly, parity breaking through octupole deformation is essential to describe asymmetric fission fragment distributions. Triaxiality, for example, has been shown to lower the inner barrier of actinides by several MeV [65, 75]. Likewise, reflection-asymmetric (octupole) degrees of freedom are necessary to reproduce mass-asymmetric fission in heavy nuclei.

Recent computational developments have made possible fully symmetry-unrestricted HFB and TDDFT calculations, in which all spatial and time-reversal symmetries can be broken if energetically favourable [65, 67]. Codes such as `HFODD` and `Sky3D` implement three-dimensional solvers capable of describing triaxial, octupole, and time-odd components of the density matrix. These advances have revealed new fission pathways, scission configurations, and fragment-spin correlations inaccessible to axially symmetric models.

In summary, microscopic theories based on DFT and its extensions offer a self-consistent foundation for the description of nuclear fission. They provide direct access to the interplay between shell effects, pairing, and deformation, which determine the shape evolution from the ground state to scission.

2 | State of the art, objectives and methods

2.1. State of the art and motivation

The need to account for nuclear deformations has been highlighted in chapter 1, particularly in regard to heavy nuclei and the fission process in section 1.4. The solution of the many-body problem has always been a computational challenge, mainly mitigated by using expansions on bases and/or assuming certain symmetries to reduce the dimensionality of the problem. The problems that arise when using either of the aforementioned approaches call for the implementation of unconstrained codes.

Basis expansions An efficient method to solve the many-body problem is to use basis expansions of the harmonic oscillator, similar to the nuclear system as mentioned in section 1.1. Several implement this kind of procedure, one of which is used in the present work to benchmark our own implementation in section 6.1.1. The main limitation of such approach is that weakly bound states and large deformations are not well represented, the former due fundamentally different asymptotic behaviours for $r \to \infty$, between the HO – e^{-r^2} – and loosely bound or quasi-resonant states – e^{-r} [23, 71], while the latter needs a large number of HO shells to converge, leading to an exponential increase of the computational cost [47].

Symmetry assumptions Another approach to reduce the complexity of the procedure is to assume certain symmetries, as to reduce the dimensionality of the problem to save computational time. The main example of such codes is the spherical solution [19, 73] of the Hartree-Fock equations, but axially symmetric ones exist as well [53]. The limitations of such codes are obvious, as they systematically prevent the representation of certain broken symmetries.

Unconstrained codes In recent years, codes that solve the Hartree-Fock or Hartree-Fock-Bogoliubov problem on an unconstrained 3D mesh have been developed [18, 49, 59, 60]. These codes are able to represent broken symmetries, but they require a huge amount of computational power to be run at an acceptable accuracy, unless certain assumptions are made, such as plane reflection [59, 60]. Hence, the need to explore new, more computationally efficient methods to solve the many-body problem, as done in this thesis through the use of the General Conjugate Gradient method, detailed in section 4.2.3.

2.2. Objectives

The aim of this work is to develop a new implementation of the Hartree-Fock method on an unconstrained 3D mesh, by the use of the General Conjugate Gradient method. The goals addressed by this work are the following:

- assess the feasibility of the General Conjugate Gradient for the solution of large-scale eigenvalue problems;
- solve the self-consistent Hartree-Fock equations on an unconstrained 3D mesh;
- verify the numerical accuracy of the new implementation against existing spherical codes;
- gauge the numerical accuracy of deformations, comparing results with well established deformed codes; and
- attempt to produce novel results that specifically require an unconstrained implementaiton of this kind, and establish the advance brought to the field by this work.

2.3. Methods

The methods used in this work are the following:

Skyrme energy functional The many-body problem is treated within the well established Hartree-Fock framework, detailed in section 3.1; as mentioned in the introduction in chapter 1, it is not sufficient, as a more general energy density functional approach has to be taken, which is developed in section 3.3 for the Skyrme functional used in this work.

Finite differences and General Conjugate Gradient After the main equations to be solved have been derived, the numerical methods used to solve them are detailed in chapter 4, starting with the numerical discretization of the equations in section 4.1 and

then solving the eigenvalue problem using an implementation of the General Conjugate Gradient method in section 4.2.3. Finally closing with some remarks about specific details about the code and the algorithm parameters in section 4.3.

3 | Energy functional

3.1. Hartree-Fock theory

While a phenomenological description of bulk nuclear structure properties can be carried out using the liquid drop model or empirical mean-field potentials like Woods-Saxon or Nilsson, as we have seen in section 1.1, this is not sufficient to accurately reproduce all experimental ground state observables, systematically throughout the chart of nuclei, in an accurate manner.
A more rigorous approach needs to take into account the fact that the mean field which the nucleons interact with, is generated by the nucleons themselves. Starting from the many-body hamiltonian of the system, we will be able to extract a single particle Hamiltonian, including an effective mean field potential generated by the effective microscopic force, through the use of the Hartree-Fock method.
We start by writing the many-body hamiltonian of the system, which is a collection of A interacting fermions, given by

$$\hat{H} = \hat{T} + \hat{V} = \sum_i -\frac{\hbar^2}{2m}\nabla_i^2 + \sum_{i<j} v_{ij}^{(2)} + \sum_{i<j<k} v_{ijk}^{(3)} + \dots \tag{3.1}$$

The corresponding Schrödinger equation reads

$$\hat{H}\Psi = E\Psi. \tag{3.2}$$

3.1.1. Variational principle

Since $\hat{H}$ is a many body operator, finding its eigenstates would be a rather challenging task. To our aid, comes the variational principle, from which we can show that equation (3.2) is equivalent to

$$\delta E[\Psi] = \delta \frac{\langle \Psi | \, E \, | \Psi \rangle}{\langle \Psi | \Psi \rangle} = 0. \tag{3.3}$$

The variation (3.3) can be obtained from an arbitrary variation of Ψ, which can be done indipendently on $\langle\Psi|$ and $|\Psi\rangle$, since Ψ is complex, yielding

$$\langle\delta\Psi|\,\hat{H}-E\,|\Psi\rangle+\langle\Psi|\,\hat{H}-E\,|\delta\Psi\rangle=0 \tag{3.4}$$

since the variation is arbitrary, we can multiply by a phase factor $|\delta\Psi\rangle\mapsto i\,|\delta\Psi\rangle$ and get

$$-i\,\langle\delta\Psi|\,\hat{H}-E\,|\Psi\rangle+i\,\langle\Psi|\,\hat{H}-E\,|\delta\Psi\rangle=0. \tag{3.5}$$

Combining equations (3.4) and (3.5), we get

$$\langle\delta\Psi|\,\hat{H}-E\,|\Psi\rangle=0. \tag{3.6}$$

Again, since the variation is arbitrary, equation (3.6) satisfies equation (3.2).

Ground state

Since we always restrict ourselves to a certain subspace of the full Hilbert space, we can only find an approximate solution to the eigenvalue problem. Expanding this solution on the complete set of exact eigenstates of $\hat{H}$, we have

$$|\Psi\rangle=\sum_n a_n\,|\Psi_n\rangle \tag{3.7}$$

the total energy amounts to

$$E[\Psi]=\frac{\sum_{nn'}\langle a_{n'}\Psi_{n'}|\,\hat{H}\,|a_n\Psi_n\rangle}{\sum_{nn'}\langle a_{n'}\Psi_{n'}|a_n\Psi_n\rangle}=\frac{\sum_n E_n|a_n|^2}{\sum_n|a_n|^2}\geq\frac{\sum_n E_0|a_n|^2}{\sum_n|a_n|^2}\geq E_0, \tag{3.8}$$

where E_0 is the ground state energy of the system. The orthonormality of the Hamiltonian eigenfunctions $\langle\Psi_{n'}|\Psi_n\rangle=\delta_{nn'}$ has been used. Equation (3.8) tells us that the minimum of the functional $E[\Psi]$ in any variationl subspace we are considering is bound from below by the true ground state energy.

3.1.2. Hartree-Fock equations

The Hartree-Fock method is the application of the variational principle (3.6) to a system of independent particles, whose wavefunction takes the form of a Slater determinant,

which reads

$$\Psi = \frac{1}{\sqrt{A!}} \sum_{\{p\}} (-1)^p \varphi_{p(1)}(\boldsymbol{r}_1) \dots \varphi_{p(A)}(\boldsymbol{r}_A) \tag{3.9}$$

where φ_i are the single-particle orthonormal states, which serve the role of variational parameters in Hartree-Fock. The Slater determinant sums over all possible permutations of the A fermions on the single particle states, with a $-$ sign according to the parity of the permutation. The Slater determinant statisfies the permutation symmetry of fermions, so that the Pauli exclusion principle is not violated.
To ensure the orthonormality of the single-particle states, we need to add a Lagrange multiplier to the variation (3.6) of E, which ends up reading

$$\delta\left(E[\Psi] - \sum_i \lambda_i \int \varphi_i^* \varphi_i d\boldsymbol{r} \right) = 0. \tag{3.10}$$

The total energy of the system is given by

$$E[\Psi] = \langle \Psi | \, \hat{T} + \hat{V} \, | \Psi \rangle = \langle \Psi | \, \hat{T} \, | \Psi \rangle + \langle \Psi | \, \hat{V} \, | \Psi \rangle \,, \tag{3.11}$$

which can be expressed through the single-particle states $\{\varphi_i\}$, yielding

$$\langle \Psi | \, \hat{T} \, | \Psi \rangle = \sum_i^A -\frac{\hbar^2}{2m} \int \varphi_i^*(\boldsymbol{r}) \nabla^2 \varphi_i(\boldsymbol{r}) d\boldsymbol{r} = \sum_i \langle i | \, t \, | i \rangle \tag{3.12}$$

$$\langle \Psi | \, \hat{V} \, | \Psi \rangle = \frac{1}{2} \sum_{ij} \int \varphi_i^*(\boldsymbol{r}) \varphi_j^*(\boldsymbol{r'}) v_{ij}(\boldsymbol{r}, \boldsymbol{r'}) \varphi_i(\boldsymbol{r}) \varphi_j(\boldsymbol{r'}) d\boldsymbol{r} d\boldsymbol{r'} \tag{3.13}$$

$$- \frac{1}{2} \sum_{ij} \int \varphi_i^*(\boldsymbol{r}) \varphi_j^*(\boldsymbol{r'}) v_{ij}(\boldsymbol{r}, \boldsymbol{r'}) \varphi_i(\boldsymbol{r'}) \varphi_j(\boldsymbol{r}) d\boldsymbol{r} d\boldsymbol{r'} \tag{3.14}$$

$$= \frac{1}{2} \langle ij | \, \overline{v} \, | ij \rangle \,. \tag{3.15}$$

If we use $\varphi_i^*(\boldsymbol{r})$ as the quantity to be varied in equation (3.10), we get the *Hartree-Fock equations*

$$- \frac{\hbar^2}{2m} \nabla^2 \varphi_i \tag{3.16}$$

$$+ \frac{1}{2} \sum_j^A \int \varphi_j^*(\mathbf{r'}) v_{ij}(\mathbf{r}, \mathbf{r'}) \, \varphi_j(\mathbf{r'}) \, \varphi_i(\mathbf{r}) \, d\mathbf{r'} \tag{3.17}$$

$$- \frac{1}{2} \sum_j^A \int \varphi_j^*(\mathbf{r'}) \, v_{ij}(\mathbf{r}, \mathbf{r'}) \, \varphi_j(\mathbf{r}) \, \varphi_i(\mathbf{r'}) \, d\mathbf{r'} = h\varphi_i = \varepsilon_i \varphi_i \tag{3.18}$$

here the Lagrange multipliers λ_i have been replaced by ε_i, since they can be interpreted as the energy of the single-particle states.
Now, a couple of remarks are in order.

Exchange interaction The first interaction term (3.17), called Hartree term, arises from considering independent particles, and is also routinely found in classical physics. The second one in (3.18), called Fock term, or exchange term, takes the form of an integral operator and is present when considering quantum mechanical indistinguishable particles. For what concerns the solution of equation (3.16), the Fock term is problematic, and can be avoided using zero-range forces like the Skyrme one [68], which is used in the present work, since it renders the exchange term as a local one.

Self-consistent solution Even if the interaction terms are local, the equation is still highly non-linear, since the mean field potential will be a function of the eigenfunctions themselves. The consequece is that the solution needs to be found *self-consistently*, that is, by solving for the set of eigenfunctions $\{\varphi_i\}$, using them to build the new mean field, and solving again, repeating the process until convergence.

3.1.3. Symmetries in Hartree-Fock

Since the objective of this work is to solve the Hartree-Fock equations without spatial symmetry assumptions, it is useful to first understand how symmetries propagate along the self-consistent calculation.
We start by defining the creation and annihilation operators of the single particle hamiltonian eigenstates, $a_i^\dagger, a_i$, which abide the usual anticommutation relations of fermions

$$\{a_i, a_j^\dagger\} = \delta_{ij} \tag{3.19}$$

If we expand on a different, orthonormal complete basis $\{\chi_l\}$, we can write the corresponding creation and annihilation operators $c_l^\dagger, c_l$ as

$$\varphi_k = \sum_l D_{lk}\chi_l \tag{3.20}$$

$$a_k^\dagger = \sum_l D_{lk}c_l^\dagger \tag{3.21}$$

$$a_k = \sum_l D_{lk}^\dagger c_l \tag{3.22}$$

Since orthonormality is guaranteed for both sets, taking $\langle\varphi_j|\varphi_k\rangle$ yields

$$\delta_{jk} = \langle\varphi_j|\varphi_k\rangle = \sum_{ll'} D^\dagger_{l'j} D_{lk} \langle\chi_l|\chi'_l\rangle \implies DD^\dagger = 1, \tag{3.23}$$

meaning that D is a unitary transformation. We can define the density matrix as

$$\rho_{ll'} = \langle\Psi| c^\dagger_{l'} c_l |\Psi\rangle , \tag{3.24}$$

whose trace is equal to the particle number A, as per equation (3.25)

$$\operatorname{Tr}\rho = \sum_{ll} \langle\Psi| c^\dagger_l c_l |\Psi\rangle = \sum_{ll} \langle\Psi| a^\dagger_l a_l |\Psi\rangle = \sum_{ll}^{A} \langle\Psi|\Psi\rangle = A. \tag{3.25}$$

Writing the many body hamiltonian (3.2) in the arbitrary basis of second quantization operators $c^\dagger_l, c_l$, we get

$$\hat{H} = \sum_{l_1 l_2} t_{l_1 l_2} c^\dagger_{l_1} c_{l_2} + \frac{1}{4} \sum_{l_1 l_2 l_3 l_4} \overline{v}_{l_1 l_2 l_3 l_4} c^\dagger_{l_1} c^\dagger_{l_2} c_{l_3} c_{l_4} \tag{3.26}$$

where $t_{l_1 l_2}$ and $\overline{v}_{l_1 l_2 l_3 l_4}$ are defined as

$$t_{l_1 l_2} = \langle -| c_{l_1} c_{l_2} t c^\dagger_{l_1} c^\dagger_{l_2} |-\rangle = \langle l_1 l_2| t |l_1 l_2\rangle \tag{3.27}$$

$$\overline{v}_{l_1 l_2 l_3 l_4} = \langle l_1 l_2 l_3 l_4| v |l_1 l_2 l_3 l_4\rangle - \langle l_1 l_2 l_4 l_3| v |l_1 l_2 l_4 l_3\rangle . \tag{3.28}$$

The minimization (3.10) can be restated as the variation of $\langle\Psi| \hat{H} |\Psi\rangle$, with respect to the density matrix $\rho_{ll'}$, which yields

$$h_{ll'} = \frac{\partial E[\rho]}{\partial \rho_{ll'}} = t + \sum_{kk'} \overline{v}_{lk'l'k} \rho_{kk'} = t + \Gamma_{ll'} \tag{3.29}$$

where $\Gamma_{ll'}$ is the mean field potential in the arbitrary basis. Being h diagonal in the Hartree-Fock basis, the self-consistent solution is the one for which

$$[h, \rho] = 0 \tag{3.30}$$

holds.

Symmetry propagation

Let us suppose to start a Hartree-Fock calculation with an initial guess for which the corresponding density matrix $\rho^{(0)}$ is symmetric under the action of a many-body symmetry operator S which commutes with the Hamiltonian

$$[S, \hat{H}] = 0. \tag{3.31}$$

It can be shown [57] that

$$S\Gamma[\rho]S^\dagger = \Gamma[S\rho S^\dagger]. \tag{3.32}$$

The single particle Hamiltonian h will then display the same property

$$Sh[\rho]S^\dagger = h[S\rho S^\dagger] = h[\rho] \tag{3.33}$$

meaning that h will be symmetric under the action of S, as well as the next iteration's density matrix $\rho^{(1)}$. The symmetry S gets propagated self-consistently until the minimum is found.
This has profound numerical implications, since the minimum energy configuration of a deformed nuclei can be reached only by starting guesses with the same broken symmetries. It can be the case that numerical noise allows to explore the full energy surface, but if one has to take into consideration the numerical cost of a bad guess, then it's still advantageous to start from a correct one in terms of symmetries.

3.1.4. Density Functional Theory

It shall be evident shortly, in section 3.3, that a more general approach to microscopic models has to be taken in order to give a satisfactory description of nuclei and nuclear matter. The method that we will briefly outline here is called Density Functional Theory (DFT).
DFT was introduced by P. Hohenberg and W. Kohn in 1964 [34], by proving two theorems. The **first** Hohenberg Kohn (HK) theorem states that the energy of a fermion system, subject to an external potential V_{ext} can be expressed solely as a functional of the particle density ρ of the system

$$E[\rho] = F[\rho] + \int V_{\text{ext}}\rho(\boldsymbol{r})d\mathbf{r}, \tag{3.34}$$

where $F[\rho]$ is a universal functional given by the type of fermions considered, while V_{ext} term is the external potential to which the system is subject to; when treating atomic nuclei, the potential is generated by the nucleons themselves, so this term will be omitted

in the following. The **second** HK theorem states that the ground state of the system is found by minimizing the functional (3.34) with respect to ρ.
HK theorems are fundamental but not constructive [20], since they do not provide a form for the functional F, which is intrinsic to the physics of the fermions at hand. A pragmatic approach to using DFT was outlined by Kohn and Sham in 1965 [38]. They proposed expressing the system as a set of non-interacting particles occupying auxiliary orbitals φ_i, which yield the particle density

$$\rho(\boldsymbol{r}) = \sum_i |\varphi_i(\boldsymbol{r})|^2 \tag{3.35}$$

and an energy functional of the form

$$E[\rho] = T[\rho] + E_H[\rho] + E_{\text{xc}}[\rho]. \tag{3.36}$$

where T is the kinetic energy, which reads

$$T[\rho] = -\frac{\hbar^2}{2m} \sum_i \varphi_i^*(\boldsymbol{r}) \nabla^2 \varphi_i(\boldsymbol{r}) \tag{3.37}$$

and E_H is the classical Hartree term, which in an electronic system may read

$$E_H[\rho] = \iint \frac{\rho(\boldsymbol{r})\rho(\boldsymbol{r}')}{|\boldsymbol{r} - \boldsymbol{r}'|} d\boldsymbol{r} d\boldsymbol{r}' \tag{3.38}$$

while E_{xc} is an unknown exchange term. In electronic systems, the Hartree term is known (3.17) and the exchange term can be approximated thanks to the compensation of its error with the one of particles correlation neglection [48]. In nuclear physics, things are more complicated, since both terms are unknown; historically, effective interactions in HF have been used to extract an effective Hamiltonian density from which an energy density functional (EDF) can be formulated, whenever a pure interaction is not sufficient to describe nuclear systems, as we shall see in section 3.3.

3.2. Pairing in Hartree-Fock theory

In this section, we will discuss the two common approaches to include nuclear pairing in the HF theory. The aim of these few pages is to provide a brief overview of how the BCS equations are derived and understand the basics of the more general Hartree-Fock-Bogoliubov theory. The former method is the most widely implemented thanks to its low complexity [12, 19, 39], while the latter, more sophisticated and advanced, is the standard

in modern codes [17, 46, 64]. We will touch on it so that the reader may appreciate in the numerical chapter the natural extension of this work to the more general Bogoliubov ansatz.

3.2.1. BCS theory

The BCS approximation, from Bardeen-Cooper-Schrieffer, is the same theory used to describe Cooper pairs in superconductivity, applied to the nuclear case. The ansatz of BCS is that nucleons are paired in states whose total angular momentum is zero, such a wavefunction can be expressed as $|JM\rangle = |00\rangle$ and reads

$$|00\rangle = \sum_{m_j} \langle jm_j j - m_j|00\rangle \, |jm_j\rangle \, |j - m_j\rangle \tag{3.39}$$

Introducing the time-reversal operator $\hat{\mathcal{T}} : t \mapsto -t$, it acts on $|00\rangle$ as

$$\hat{\mathcal{T}} \, |jm_j\rangle = \widetilde{|jm_j\rangle} = (-1)^{j+m_j} \, |j - m_j\rangle \, , \tag{3.40}$$

using this relation, equation (3.39) becomes

$$|00\rangle = -\frac{1}{\sqrt{2j+1}} \sum_{m_j} |jm_j\rangle \, \widetilde{|jm_j\rangle}. \tag{3.41}$$

Hence BCS amounts to replacing the Slater determinant with a more general wavefunction to describe the ground state, which reads

$$|\text{BCS}\rangle = \prod_{k>0} (u_k + v_k a_{\tilde{k}}^\dagger a_k^\dagger) \, |-\rangle \tag{3.42}$$

where u_k and v_k are real parameters whose meaning will shortly be clear, k is short-hand for $|jm\rangle$, and $\tilde{k} = -k$ denotes the time-reversal state of k; the product runs over positive k only. The BCS wavefunction is the creation in the vacuum of quasi-particles made of time-reversal paired particles, instead of individual ones. The normalization condition on the BCS wavefunction reads

$$1 = \langle \text{BCS}|\text{BCS}\rangle = \prod_{k>0} \langle -| \, (u_k + v_k a_k a_{\tilde{k}})(u_k + v_k a_{\tilde{k}}^\dagger a_k^\dagger) \, |-\rangle = \prod_{k>0} (u_k^2 + v_k^2) = 1 \tag{3.43}$$

which implies, for every pair k, the condition

$$u_k^2 + v_k^2 = 1. \tag{3.44}$$

Taking the expectation value of the particle number operator $\hat{N} = \sum_k a_k^\dagger a_k$ yields [8]

$$\langle \mathrm{BCS} | \hat{N} | \mathrm{BCS} \rangle = 2 \sum_{k>0} v_k^2, \tag{3.45}$$

while the expectation value of the particle number dispersion reads

$$\left\langle \Delta \hat{N}^2 \right\rangle = \left\langle \hat{N}^2 \right\rangle - \left\langle \hat{N} \right\rangle^2 = 4 \sum_{k>0} v_k^2 u_k^2. \tag{3.46}$$

The consequence of this result is profound. The BCS ansatz does not assume a fixed number of particles, rather it becomes an observable of the system, with an expectation value that depends on how the parameters v_k^2 are set, which represent the probability of finding a particle in the k-th state. We can now write the many body Hamiltonian of the system as in equation (3.26)

$$\hat{H} = \sum_{k_1 k_2} t_{k_1 k_2} a_{k_1}^\dagger a_{k_2} + \frac{1}{4} \sum_{k_1 k_2 k_3 k_4} \overline{v}_{k_1 k_2 k_3 k_4} a_{k_1}^\dagger a_{k_2}^\dagger a_{k_3} a_{k_4} \tag{3.47}$$

and replace it with the Routhian

$$\langle \mathrm{BCS} | \hat{H} - \lambda \hat{N} | \mathrm{BCS} \rangle \tag{3.48}$$

so that the expected number of particles may be fixed, under the appropriate choice of λ, by the relation

$$\frac{\partial}{\partial N} \langle \mathrm{BCS} | \hat{H} | \mathrm{BCS} \rangle = \lambda. \tag{3.49}$$

the Lagrange multiplier λ takes on the meaning of the Fermi energy. We can now apply the variational principle (3.6) to (3.48) using the v_k as variational quantities, which yields

$$4 \tilde{\varepsilon}_k^2 u_k^2 v_k^2 = \Delta_k^2 - 4 \Delta_k^2 u_k^2 v_k^2, \tag{3.50}$$

where the pairing gap Δ_k is defined as

$$\Delta_k = - \sum_{k'} \overline{v}_{k \tilde{k} k' \tilde{k}'} v_{k'} u_{k'} \tag{3.51}$$

and the quantity $\tilde{\varepsilon}_k$ is defined as

$$\tilde{\varepsilon}_k = \frac{1}{2}\left[t_{kk} + t_{\tilde{k}\tilde{k}} - 2\lambda + \sum_{k'}(\overline{v}_{k\tilde{k}k'\tilde{k}'}v_{k'}u_{k'} + \overline{v}_{\tilde{k}k'\tilde{k}k'})v_{k'}^2\right] \tag{3.52}$$

$$= \frac{1}{2}[h_{kk} + h_{\tilde{k}\tilde{k}}] - \lambda. \tag{3.53}$$

Introducing the quasi-particle energy

$$E_k = \sqrt{\tilde{\varepsilon}_k^2 + \Delta_k^2} \tag{3.54}$$

we can combine definitions (3.51) and (3.54) with equation (3.52), under the normalization condition (3.44), to get an equation for v_k^2

$$v_k^2 = \frac{1}{2} \pm \frac{|\tilde{\varepsilon}_k|}{2E_k}. \tag{3.55}$$

Since in the Hartree-Fock limit, where the occupations v_k^2 are equal to one below the fermi energy and zero above, and the gaps Δ_k vanish, rendering $E_k = \tilde{\varepsilon}_k$, we only select the solution

$$v_k^2 = \frac{1}{2} - \frac{\tilde{\varepsilon}_k}{2E_k}. \tag{3.56}$$

Using the normalization condition to write $u_k^2 = 1 - v_k^2$, and plugging it into the gaps definition (3.51), we arrive to the gap equation

$$\Delta_k = -\sum_{k'} \frac{\Delta_{k'}\overline{v}_{k\tilde{k}k'\tilde{k}'}}{2E_{k'}} \tag{3.57}$$

The system of equations (3.57, 3.44, 3.55, 3.54, 3.52), together with the condition on $\hat{N}$ – ie $\left\langle \hat{N} \right\rangle = N$ – is closed and can be solved numerically, usually through an effective pairing interaction.

3.2.2. Hartree-Fock-Bogoliubov theory

The most general ansatz to account for pairing interactions in Hartree-Fock theory is the Hartree-Fock-Bogoliubov (HFB) theory, it allows a treatment of the mean-field and pairing interactions in a unified way, the quasi-particles created on the vacuum are the most general ones, instead of being time-reversal paired particles. Let us start by writing

a Bogoliubov transformation from the particle basis c_i to a quasi-particle one

$$\beta_k^\dagger = \sum_l U_{lk} c_l^\dagger + V_{lk} c_l. \tag{3.58}$$

If we take the Hermitian conjugate of the relation (3.58), we get the transformation for β_k, we are then able to write in matrix form

$$\begin{pmatrix} \beta \\ \beta^\dagger \end{pmatrix} = \begin{pmatrix} U^\dagger & V^\dagger \\ V^T & U^T \end{pmatrix} \begin{pmatrix} c \\ c^\dagger \end{pmatrix} = \mathcal{W}^\dagger \begin{pmatrix} c \\ c^\dagger \end{pmatrix}, \tag{3.59}$$

where the matrix of matrices $\mathcal{W}$ reads

$$\mathcal{W} = \begin{pmatrix} U & V^* \\ V & U^* \end{pmatrix}. \tag{3.60}$$

Taking the product $\mathcal{W}^\dagger\mathcal{W}$ and imposing separate fermionic commutation relations of the operators $\beta, \beta^\dagger, c, c^\dagger$, we get that $\mathcal{W}$ is unitary, hence

$$\mathcal{W}^\dagger\mathcal{W} = \mathcal{W}\mathcal{W}^\dagger = I. \tag{3.61}$$

We can now invert equation (3.59) by multiplying both sides on the left by $\mathcal{W}$, which yields

$$\mathcal{W} \begin{pmatrix} \beta \\ \beta^\dagger \end{pmatrix} = \begin{pmatrix} c \\ c^\dagger \end{pmatrix}.$$

Using the Messiah-Bloch decomposition [22], we can write the unitary matrix $\mathcal{W}$ as

$$\mathcal{W} = \begin{pmatrix} D & 0 \\ 0 & D^* \end{pmatrix} \begin{pmatrix} \overline{U} & \overline{V} \\ \overline{V} & \overline{U} \end{pmatrix} \begin{pmatrix} C & 0 \\ 0 & C^* \end{pmatrix} \tag{3.62}$$

where D and C are unitary matrices and $\overline{U}$ and $\overline{V}$ are real matrices, which have a particular blocked form, expressed through the coefficents u_k, v_k; the reader may refer to appendix A.4 for the explicit representation. We can also define the matrices U, V as

$$U = D\overline{U}C, \quad V = D^*\overline{V}C. \tag{3.63}$$

Using the decomposition (3.62) we can define the *canonical basis* as

$$a_k^\dagger = \sum_l D_{lk}^\dagger c_l^\dagger, \tag{3.64}$$

a *special Bogoliubov transformation* between *paired* levels as

$$\alpha_k^\dagger = u_k a_k^\dagger - v_k a_{\tilde{k}}, \tag{3.65}$$
$$\alpha_{\tilde{k}}^\dagger = u_k a_{\tilde{k}}^\dagger + v_k a_k, \tag{3.66}$$

and *blocked* levels

$$\alpha_i = a_i, \quad \alpha_n^\dagger = a_n^\dagger \tag{3.67}$$
$$\alpha_i = a_i^\dagger, \quad \alpha_n = a_n, \tag{3.68}$$

where $u_k = u_{\tilde{k}},\ v_k = -v_{\tilde{k}}$, and a unitary transformation of the quasi-particle operators $\alpha_k^\dagger$ among themselves

$$\beta_k^\dagger = \sum_{k'} C_{k'k} a_{k'}^\dagger. \tag{3.69}$$

We are now able to define the Bogoliubov ground state $|\mathrm{HFB}\rangle$, as the one for which

$$\beta_k \left|\mathrm{HFB}\right\rangle = 0 \ \forall k = 1, \ldots, M \tag{3.70}$$

where M is determined by the physical situation [57]. The wavefunction that satisfies this condition reads

$$\left|\mathrm{HFB}\right\rangle = \prod_k^M \beta_k \left|-\right\rangle. \tag{3.71}$$

We can define the pairing tensor as

$$\kappa_{ll'} = \left\langle \mathrm{HFB}\right| c_{l'} c_l \left|\mathrm{HFB}\right\rangle, \tag{3.72}$$

which in matrix form reads, alongside the density matrix

$$\kappa = UV^\dagger, \quad \rho = V^* V^T. \tag{3.73}$$

We can now apply the variational principle (3.6)

$$\delta \frac{\left\langle \mathrm{HFB}\right| \hat{H} - \lambda \hat{N} \left|\mathrm{HFB}\right\rangle}{\left\langle \mathrm{HFB}|\mathrm{HFB}\right\rangle} = 0. \tag{3.74}$$

which yields the eigenvalue problem

$$\begin{pmatrix} h - \lambda & \Delta \\ -\Delta^* & -(h-\lambda)^* \end{pmatrix} \begin{pmatrix} U_k \\ V_k \end{pmatrix} = \mathcal{H}_{\mathrm{HFB}} \begin{pmatrix} U_k \\ V_k \end{pmatrix} = E_k \begin{pmatrix} U_k \\ V_k \end{pmatrix}, \tag{3.75}$$

Here, h is the single-particle Hamiltanian, which reads

$$h_{kk'} = t_{kk'} + \Gamma_{kk'}, \tag{3.76}$$

where $\Gamma_{kk'}$ is the mean field potential, given by

$$\Gamma_{kk'} = \sum_{ll'} \overline{v}_{kl'k'l}\rho_{ll'} \tag{3.77}$$

and the pairing field Δ reads

$$\Delta_{kk'} = \sum_{ll'} \overline{v}_{kk'll'}\kappa_{ll'}. \tag{3.78}$$

In the canonical basis, we are able to solve for the occupation numbers

$$u_k^2 = \frac{1}{2}\left(1 + \frac{h_{kk} + h_{\tilde{k}\tilde{k}}}{\sqrt{(h_{kk} + h_{\tilde{k}\tilde{k}})^2 + 4\Delta_{k\tilde{k}}^2}}\right) \tag{3.79}$$

where $v_k^2 = 1 - u_k^2$ is guaranteed by the unitarity of the matrices. Starting from an initial guess, we solve the eigenvalue problem (3.75), we extract the occupation numbers (3.79), use them to build the new mean field (3.77) and pairing field (3.78), and repeat the process until convergence.

HFB quasi-particle spectrum Let us assume that $\Psi = (U,\ V)^T$ is a solution of equation (3.75) with eigenvalue E

$$\mathcal{H}_{\text{HFB}}\Psi = E\Psi. \tag{3.80}$$

Let the particle-hole matrix $\mathcal{C}$ be defined as

$$\mathcal{C} = \begin{pmatrix} 0 & I \\ I & 0 \end{pmatrix}, \tag{3.81}$$

it's trivial to show that

$$\mathcal{C}\mathcal{H}_{\text{HFB}}\mathcal{C} = -\mathcal{H}_{\text{HFB}}^*, \tag{3.82}$$

and

$$\mathcal{C} = \mathcal{C}^{-1} \implies \mathcal{C}\mathcal{H}_{\text{HFB}} = -\mathcal{H}_{\text{HFB}}^*\mathcal{C}. \tag{3.83}$$

If we take the complex conjugate of equation (3.80), we get

$$\mathcal{H}^*_{\mathrm{HFB}}\Psi^* = E\Psi^*, \tag{3.84}$$

if we multiply both sides on the left by $\mathcal{C}$ and use (3.83), we get

$$-\mathcal{H}_{\mathrm{HFB}}\mathcal{C}\Psi^* = E\mathcal{C}\Psi^*, \tag{3.85}$$

$$\mathcal{H}_{\mathrm{HFB}}\mathcal{C}\Psi^* = -E\mathcal{C}\Psi^*, \tag{3.86}$$

meaning that $\mathcal{C}\Psi^*$ is a solution of the eigenvalue problem (3.75) as well, with eigenvalue $-E$, hence for every quasi-particle energy we have a corresponding opposite-sign one; moreover, it can be proven that the HFB hamiltonian is unbounded, both from below and above [54]. This feature poses a challenge for numerical solutions of the HFB problem, as we shall see in chapter 4.

3.3. Skyrme

Now that the theoretical framework is clear, we can use the Skyrme microscopic effective interaction to do nuclear structure calculations.

3.3.1. Skyrme force

It was first proposed by Tony Skyrme in 1958 [68] as a zero range force between nucleons, comprising a two body attractive term that reads

$$\begin{aligned} v^{(2)}(\mathbf{r}_1,\mathbf{r}_2) = {} & t_0\left(1+x_0P_\sigma\right)\delta(\mathbf{r}) \\ & + \frac{1}{2}t_1\left(1+x_1P_\sigma\right)\left[\mathbf{P}'^2\delta(\mathbf{r}) + \delta(\mathbf{r})\mathbf{P}^2\right] \\ & + t_2P_\sigma\mathbf{P}'\cdot\delta(\mathbf{r})\mathbf{P} \\ & + iW_0\boldsymbol{\sigma}\cdot\left[\mathbf{P}'\times\delta(\mathbf{r})\mathbf{P}\right] \end{aligned}$$

and a three body term, that is

$$v^{(3)}(\boldsymbol{r}_1,\boldsymbol{r}_2,\boldsymbol{r}_3) = t_3\delta(\boldsymbol{r}_1-\boldsymbol{r}_2)\delta(\boldsymbol{r}_2-\boldsymbol{r}_3)$$

which mimics the repulsive three-body force; without it, a collapse of the nuclear density would occur. The different operators are defined as

$$\mathbf{r} = \mathbf{r}_1 - \mathbf{r}_2 \quad \mathbf{R} = \frac{\mathbf{r}_1 + \mathbf{r}_2}{2} \tag{3.87}$$

which are respectively the relative position of two particles and their center of mass coordinate, assuming equal masses.

$$\mathbf{P} = \frac{-i(\nabla_1 - \nabla_2)}{2} \tag{3.88}$$

which is the so called relative wave-number operator, corresponding to the relative momentum of the two interacting particles.

$$\boldsymbol{\sigma} = \boldsymbol{\sigma}_1 + \boldsymbol{\sigma}_2 \tag{3.89}$$

being the total spin of the two interacting particles, and lastly

$$\mathbf{P}_\sigma = \frac{(1 + \boldsymbol{\sigma}_1 \cdot \boldsymbol{\sigma}_2)}{2} \tag{3.90}$$

which represents the spin-exchange operator. Primed operators refer to the adjoint acting on the left.
It's trivial to show that the three-body term, in the case of even-even nuclei, is equivalent to a two-body, density-dependent interaction [73]

$$v^{(3)}(\boldsymbol{r}_1, \boldsymbol{r}_2) = \frac{1}{6} t_3 (1 + P_\sigma) \delta(\boldsymbol{r}) \rho(\boldsymbol{R}) \tag{3.91}$$

The zero-range feature is apparent in the choice of the Dirac delta $\delta(\mathbf{r})$, which allows the writing of the Fock term detailed in (3.18) as a purely local one.

Modern parametrization

The Skyrme force has evolved from the original one to accomodate new nuclei and properties, done through the addition of a few parameters, yielding the following form of the

interaction [14]

$$\begin{aligned} v^{(2)}(\mathbf{r}_1,\mathbf{r}_2) = & \, t_0\,(1+x_0P_\sigma)\,\delta(\mathbf{r}) \\ & + \frac{1}{2}t_1\,(1+x_1P_\sigma)\left[\mathbf{P}'^2\delta(\mathbf{r}) + \delta(\mathbf{r})\mathbf{P}^2\right] \\ & + t_2\,(1+x_2P_\sigma)\,\mathbf{P}'\cdot\delta(\mathbf{r})\mathbf{P} \\ & + \frac{1}{6}t_3\,(1+x_3P_\sigma)\,[\rho(\mathbf{R})]^\sigma\,\delta(\mathbf{r}) \\ & + iW_0\boldsymbol{\sigma}\cdot[\mathbf{P}'\times\delta(\mathbf{r})\mathbf{P}] \\ & + \frac{1}{6}t_3\,(1+x_3P_\sigma)\,[\rho(\mathbf{R})]^\sigma\,\delta(\mathbf{r}) \end{aligned}$$

Here, the boundary between Hartree-Fock and DFT starts to thin out, as the exponent σ of the density makes that piece of the force a true three-body interaction only for the value $\sigma = 1$ [26]. On top of that, additional, empirical tuning of the resulting energy density needed to reach satisfactory physical accuracy, such as the case for the spin-orbit couplings [56], prompts for the following, well established proceeding: use the Skyrme interaction to obtain the Hamiltonian density

$$\langle H\rangle = \langle\Psi|\,H\,|\Psi\rangle = \int \mathcal{H}(\boldsymbol{r})d\mathbf{r} \tag{3.92}$$

and use it as a starting point to build an energy density functional and employ DFT.

3.3.2. Energy density functional

The energy functional to be minimized is of the form [3]

$$E_{\mathrm{HF}} = E_{\mathrm{Kin}} + E_{\mathrm{Skyrme}} + E_{\mathrm{Coul}} = \int (\mathcal{E}_{\mathrm{Kin}} + \mathcal{E}_{\mathrm{Skyrme}} + \mathcal{E}_{\mathrm{Coul}})d\boldsymbol{r}. \tag{3.93}$$

Densities

Functional (3.93) can be expressed through a series of particle densities. Let us define them and express them on the spin coordiantes up ($\uparrow$) and down ($\downarrow$) for the convinience in a mesh representation.

The starting point is the density matrix, defined as

$$\rho_q(\mathbf{r}\sigma,\mathbf{r}\sigma') = \sum_\alpha \phi_{\alpha,\sigma}(\mathbf{r})\phi^*_{\alpha,\sigma'}(\mathbf{r}') \tag{3.94}$$

where the index α goes through all single particle states of the particles of type q (protons, neutrons) and the index σ refers to the spin coordinate. The particle density is defined

as

$$\rho_q(\mathbf{r}) \coloneqq \rho_q(\mathbf{r},\mathbf{r}')\Big|_{\mathbf{r}=\mathbf{r}'} \coloneqq \sum_\sigma \rho(\mathbf{r}\sigma,\mathbf{r}'\sigma)\Big|_{\mathbf{r}=\mathbf{r}'} = \sum_\alpha \phi_\uparrow(\mathbf{r})\phi_\uparrow^*(\mathbf{r}') + \phi_\downarrow(\mathbf{r})\phi_\downarrow^*(\mathbf{r}')\Big|_{\mathbf{r}=\mathbf{r}'}$$
$$= \sum_\alpha |\phi_\uparrow(\mathbf{r})|^2 + |\phi_\downarrow(\mathbf{r})|^2. \tag{3.95}$$

The kinetic density reads

$$\begin{aligned}\tau_q(\mathbf{r}) &\coloneqq \sum_\alpha \nabla'\cdot\nabla\rho_q(\mathbf{r},\mathbf{r}')\Big|_{\mathbf{r}'=\mathbf{r}} \\ &= \sum_{\sigma,\alpha} \nabla\phi_\sigma(\mathbf{r})\cdot\nabla\phi_\sigma^*(\mathbf{r}')\Big|_{\mathbf{r}=\mathbf{r}'} = \sum_{\sigma,\alpha}|\nabla\phi_\sigma(\mathbf{r})|^2 \\ &= \sum_\alpha |\nabla\phi_\uparrow(\mathbf{r})|^2 + |\nabla\phi_\downarrow(\mathbf{r})|^2.\end{aligned} \tag{3.96}$$

The spin density reads

$$s_q(\mathbf{r},\mathbf{r}') \coloneqq \sum_{\sigma\sigma',i} \rho_q(\mathbf{r}\sigma,\mathbf{r}'\sigma')\,\langle\sigma'|\,\hat{\boldsymbol{\sigma}}\,|\sigma\rangle = \sum_\alpha \begin{bmatrix}\phi_\uparrow^*(\mathbf{r}') & \phi_\downarrow^*(\mathbf{r}')\end{bmatrix}\hat{\boldsymbol{\sigma}}\begin{bmatrix}\phi_\uparrow(\mathbf{r})\\ \phi_\downarrow(\mathbf{r})\end{bmatrix} \tag{3.97}$$

and lastly, the spin-orbit density tensor reads

$$\begin{aligned}J_{q,\mu\nu} &\coloneqq \frac{1}{2i}(\partial_\mu - \partial'_\mu)s_{q,\nu}(\mathbf{r},\mathbf{r}')\Big|_{\mathbf{r}'=\mathbf{r}} \\ &= \frac{1}{2i}\left(\begin{bmatrix}\phi_\uparrow^*(\boldsymbol{r}') & \phi_\downarrow^*(\boldsymbol{r}')\end{bmatrix}\partial_\mu\hat{\sigma}_\nu\begin{bmatrix}\phi_\uparrow(\mathbf{r})\\ \phi_\downarrow(\mathbf{r})\end{bmatrix} - \begin{bmatrix}\phi_\uparrow(\boldsymbol{r}) & \phi_\downarrow(\boldsymbol{r})\end{bmatrix}\partial'_\mu\hat{\sigma}_\nu\begin{bmatrix}\phi_\uparrow^*(\mathbf{r}')\\ \phi_\downarrow^*(\mathbf{r}')\end{bmatrix}\right)_{\mathbf{r}'=\mathbf{r}} \\ &= \sum_\alpha \mathrm{Im}\left\{\begin{bmatrix}\phi_\uparrow^*(\boldsymbol{r}) & \phi_\downarrow^*(\boldsymbol{r})\end{bmatrix}\partial_\mu\hat{\sigma}_\nu\begin{bmatrix}\phi_\uparrow(\mathbf{r})\\ \phi_\downarrow(\mathbf{r})\end{bmatrix}\right\}\end{aligned} \tag{3.98}$$

which also defines the spin-orbit current vector $\boldsymbol{J}$ that reads

$$J_{q,\kappa}(\boldsymbol{r}) = \sum_{\mu\nu}\epsilon_{\kappa\mu\nu}J_{q,\mu\nu}(\boldsymbol{r}). \tag{3.99}$$

Kinetic functional

The kinetic term can be expressed as

$$\mathcal{E}_{\mathrm{Kin}} = \frac{\hbar^2}{2m}\tau \tag{3.100}$$

which is found integrating by parts (3.37).

Skyrme functional

Since this work only deals with even-even nuclei, only time-even densities, which are the ones previously defined, are non-vanishing, due to the ground state being time-reversal invariant [3]. This reduces the Skyrme functional to the following form [70]

$$\mathcal{E}_{\text{Skyrme}} = \sum_{t=0,1} \left\{ C_t^{\rho}[\rho_0]\rho_t^2 + C_t^{\Delta\rho}\rho_t\nabla^2\rho_t + C_t^{\nabla\cdot J}\rho_t\nabla\cdot\mathbf{J}_t + C_t^{\tau}\rho_t\tau_t \right\} \tag{3.101}$$

where

$$C_0^{\rho} = +\frac{3}{8}t_0 + \frac{3}{48}t_3\rho_0^{\sigma} \tag{3.102}$$

$$C_1^{\rho} = -\frac{1}{8}t_0(1+2x_0) - \frac{1}{48}t_3(1+x_3)\rho_0^{\sigma} \tag{3.103}$$

$$C_0^{\tau} = +\frac{3}{16}t_1 + \frac{1}{16}t_2(5+4x_2) \tag{3.104}$$

$$C_1^{\tau} = -\frac{1}{16}t_1(1+2x_1) + \frac{1}{16}t_2(1+2x_2) \tag{3.105}$$

$$C_0^{\Delta\rho} = -\frac{9}{64}t_1 + \frac{1}{64}t_2(5+4x_2) \tag{3.106}$$

$$C_1^{\Delta\rho} = +\frac{3}{64}t_1(1+2x_1) + \frac{1}{64}t_2(1+2x_2) \tag{3.107}$$

$$C_0^{\nabla\cdot J} = -\frac{3}{4}W_0 \tag{3.108}$$

$$C_1^{\nabla\cdot J} = -\frac{1}{4}W_0. \tag{3.109}$$

Here, $t = 0, 1$ refers to the isoscalar and isovector components of the densities, eg

$$\rho_0 = \rho_p + \rho_n$$
$$\rho_1 = \rho_p - \rho_n.$$

We can now derive the Kohn-Sham equations, by minimizing the functional under the constraint

$$\langle\varphi_i|\varphi_j\rangle = \delta_{ij}. \tag{3.110}$$

The resulting Kohn-Sham equations are of the form

$$\left[-\nabla\left(\frac{\hbar^2}{2m_q^*(\mathbf{r})}\nabla\right) + U_q(\mathbf{r}) + \delta_{\text{q,proton}}U_C(\mathbf{r}) - i\mathbf{B}_q(\mathbf{r})\cdot(\nabla\times\boldsymbol{\sigma})\right]\varphi_\alpha = \varepsilon_\alpha\varphi_\alpha \tag{3.111}$$

where an effective mass field arises, which is defined as

$$\frac{\hbar^2}{2m_q^*(\mathbf{r})} = \frac{\delta\mathcal{E}}{\delta\tau_q} \tag{3.112}$$

a mean field potential, which reads

$$U_q(\mathbf{r}) = \frac{\delta\mathcal{E}}{\delta\rho_q} \tag{3.113}$$

and a spin-orbit field, given by

$$\mathbf{B}_q(\mathbf{r}) = \frac{\delta\mathcal{E}}{\delta\mathbf{J_q}}. \tag{3.114}$$

The coulomb field U_C, which is present only in the single particle equation for protons, doesn't come from the Skyrme interaction, rather from the Coulomb part of the whole functional. It will be properly derived in section 3.4.
Following the rules for functional derivatives, outlined in the appendix A.3 we get

$$\begin{aligned}\frac{\hbar^2}{2m_q^*(\mathbf{r})} = &+ \frac{\hbar^2}{2m} \\ &+ \frac{1}{8}[t_1(2+x_1) + t_2(2+x_2)]\rho(\mathbf{r}) \\ &- \frac{1}{8}[t_1(1+2x_1) + t_2(1+2x_2)]\rho_q(\mathbf{r})\end{aligned} \tag{3.115}$$

$$\begin{aligned}U_q(\mathbf{r}) = &+ \frac{1}{8}[t_1(2+x_1) + t_2(2+x_2)]\rho \\ &+ \frac{1}{8}[t_2(1+2x_2) - t_1(1+2x_1)]\rho_q \\ &+ \frac{1}{8}[t_1(2+x_1) + t_2(2+x_2)]\tau \\ &+ \frac{1}{8}[t_2(1+2x_2) - t_1(1+2x_1)]\tau_q \\ &+ \frac{1}{16}[t_2(2+x_2) - 3t_1(2+x_1)]\nabla^2\rho \\ &+ \frac{1}{16}[3t_1(2x_1+1) + t_2(2x_2+1)]\nabla^2\rho_q\end{aligned} \tag{3.116}$$

$$\begin{aligned}\mathbf{B}_q(\mathbf{r}) = &+ \frac{1}{2}W_0[\nabla\rho + \nabla\rho_q] \\ &- \frac{1}{8}(t_1x_1 + t_2x_2)\mathbf{J} + \frac{1}{8}(t_1 - t_2)\mathbf{J}_q.\end{aligned} \tag{3.117}$$

Unless otherwise specified, unlabelled densities denote isoscalar quantities (sum of neutron and proton).

3.3.3. Functionals

The set of parameters $(t_0, t_1, t_2, t_3, x_0, x_1, x_2, \sigma, W_0)$ in the Skyrme functional (3.101) is not fixed and may vary for different parametrizations. These parameters are fitted on experimental data so that the EDF may produce accurate results.

The first parametrization was given by D Vautherin and D M Brink [73], known as S I, was fitted on double magic nuclei and nuclear matter data. This was sufficient for their calculations but not enough to describe other nuclei. Fitting these parameters on further data over the years led to the introduction of other parameter sets such as S I, S II, S III [14]. These were good functionals to reproduce ground states and certain aspects of nuclear structure, but they lacked the ability to account with good accuracy for deformation properties and fission barriers. The first modern functional to address this issue has been the SkM* [2].

Nowadays functionals such as the SLy family [15], try to be as broad as possible, taking into account results from ab-initio theories, exotic nuclei, drip lines, nuclei far from stability and so on.

3.4. Coulomb interaction

Unlike the Skyrme interaction, the Coulomb force is finite-range, giving rise to an unwanted integral operator in the single-particle Hamiltonian. A well known and widely used device is the Slater approximation [31], which gives a local exchange interaction.
In this approximation, the Coulomb energy reads

$$E_{\text{Coul}} = \int \mathcal{E}_{\text{Coul}}(\mathbf{r}) d\boldsymbol{r}$$

where the energy density is given by

$$\mathcal{E}_{\text{Coul}}(\boldsymbol{r}) = \frac{e^2}{2}\left[\int \frac{\rho_p(\mathbf{r})\rho_p(\mathbf{r}')}{|\mathbf{r}-\mathbf{r}'|} d\mathbf{r}' - \frac{3}{2}\left(\frac{3}{\pi}\right)^{\frac{1}{3}} \rho_p^{4/3}(\mathbf{r})\right]. \tag{3.118}$$

which results in the Coulomb potential field

$$U_C(\mathbf{r}) = \frac{\delta \mathcal{E}_{\text{Coul}}}{\delta \rho_p} = \frac{e^2}{2}\left[\int \frac{\rho_p(\mathbf{r}')}{|\mathbf{r}-\mathbf{r}'|} d^3\mathbf{r}' - 2\left(\frac{3}{\pi}\right)^{\frac{1}{3}} \rho_p^{1/3}(\mathbf{r})\right] \tag{3.119}$$